AIAA/AAS Astrodynamics Specialist Conference and Exhibit
16 - 19 August 2004, Providence, Rhode Island

AIAA 2004-4745

Mars Reconnaissance Orbiter Navigation[†]

Tung-Han You[*], Allen Halsell[*], Dolan Highsmith[*], Moriba Jah[§], Stuart Demcak[*], Earl Higa[*], Stacia Long[§], and Shyam Bhaskaran[*]
Jet Propulsion Laboratory, California Institute of Technology
4800 Oak Grove Drive, Pasadena, CA 91109-8099

Mars Reconnaissance Orbiter will launch in August 2005 at Cape Canaveral Air Force Station. The heavyweight spacecraft will use a Lockheed-Martin Atlas V-401 launch vehicle. It will be the first mission in a low Mars Orbit to characterize the surface, subsurface, and atmospheric properties. The intensive science operation imposes a great challenge for Navigation to satisfy the stringent requirements. This paper describes navigation key requirements, major challenges, and the sophisticated dynamic modeling. It also details the navigation strategy and processes for various mission phases. Mars Reconnaissance Orbiter will return a significant amount of scientific data in support of the objectives set by the Mars Exploration Program. A robust and precise navigation is the key to the success of this mission.

Nomenclature

I_G	=	rotation axis of inner gimbal
O_G	=	rotation axis of outer gimbal
I_θ	=	inner gimbal position in degree
O_θ	=	outer gimbal position in degree
V_{inf}	=	hyperbolic excess velocity
Φ_{SPE}	=	Sun-Probe-Earth angle
F_{solar}	=	total solar radiation force
C_{sf}	=	solar flux at 1 AU
S_{solar}	=	solar shadow scale factor
R_{sp}	=	Sun-Probe distance
A_i	=	solar pressure effective area of i^{th} spacecraft component
Ψ_i	=	illumination angle of i^{th} spacecraft component
μ_i	=	specular coefficient of i^{th} spacecraft component
ν_i	=	diffuse coefficient of i^{th} spacecraft component
β_i	=	fraction of total photons reflected from the surface of i^{th} spacecraft component
γ_i	=	fraction of photon reflected diffusively from the surface of i^{th} spacecraft component
κ_i	=	thermal emissivity coefficient of i^{th} spacecraft component
$\tilde{A}_i$	=	atmosphere effective area of i^{th} spacecraft component
ρ_{atm}	=	atmosphere density
V_{sc}	=	body-fixed spacecraft velocity vector
m_j	=	exponential function of stochastic batch size and correlation time at batch j
σ_j	=	process noise at batch j
σ_{ss}	=	steady state process noise

[†] This work was performed at the Jet Propulsion Laboratory, California Institute of Technology, Pasadena, California under contract to National Aeronautics and Space Administration
[*] Senior Member of Engineering Staff, Jet Propulsion Laboratory
[§] Member of Engineering Staff, Jet Propulsion Laboratory

I. Introduction

Mars Reconnaissance Orbiter (MRO) is scheduled to launch in August 2005 from Space Launch Complex 41 at Cape Canaveral Air Force Station. The heavyweight spacecraft will use a Lockheed-Martin Atlas V-401 launch vehicle. Its mass and scale are much larger than any recent Mars missions. With six science instruments, three engineering payloads, two additional science investigations, and an off-nadir pointing capability, MRO will be the first mission in a low Mars orbit to characterize the surface, subsurface, and atmospheric properties with unprecedented quality[1]. Figure 1 illustrates the simulation of MRO passing through the Martian Polar region during the primary science phase. The intensive and complex science operation imposes a great challenge for Navigation to satisfy the stringent requirements.

Figure 1: MRO in Science Phase

This paper briefly describes the overall mission phases and navigation key requirements. It also discusses the navigation major challenges and the sophisticated dynamic modeling. Navigation analysis, strategy, and processes are detailed.

II. Mission Overview

A. Mission Description

Similar to Mars Global Surveyor (MGS) and Odyssey (ODY), MRO consists of six mission phases – launch, cruise, approach and Mars orbit insertion (Approach-MOI), aerobraking and transition, primary science, and relay phases.

A three-week launch period is selected with a minimum of one half-an-hour launch window each day. The launch period extends from August 10 to August 30, 2005. Two discrete launch azimuths in combination with three parking orbits are designed to satisfy the target specifications. The sophisticated Centaur system is capable of correcting the flight path in real-time, which minimizes the injection error. A small targeting bias will be applied so that both orbiter and upper stage meet the planetary protection requirements satisfying the probability of an impact of Mars within 10^{-4}. The orbiter aim-point bias will be removed by the first trajectory maneuver at launch plus 15 days.

During the seven-month journey to Mars, trajectory correction maneuvers (TCMs) are planned to maintain the favorable flight trajectory. A total of five TCMs are scheduled prior to MOI. The first four TCMs are to take out the injection bias, control the flight path, and clean up any earlier leftover residual errors either from maneuver execution or orbit determination. The last one, which consists of a choice between two contingency maneuvers, is a safeguard to divert the orbiter from impacting the Martian surface. In addition to performing the orbit determination and flight path control, two active dynamic calibration activities are planned to fine tune the solar radiation pressure and small force models. Many other instrument calibrations and system checkouts will occur during this time span as well[2]. Some of the activities require slewing the spacecraft to specific attitudes, which will perturb the spacecraft dynamic profile. It requires Navigation to monitor these events and take into account the perturbations in the dynamic modeling.

MOI will be the most critical event during Approach-MOI phase. The whole purpose of this in-plane maneuver is to reduce the spacecraft velocity at periapsis enough to be captured by the Mars gravity. Approximately 1000 m/s of ΔV and 25 minutes of burn time are required to complete the maneuver[3]. At two and a half weeks prior to the arrival at Mars in March 2006, Navigation will deliver the final MOI design. It will place the post-capture orbit into a 35-hour period with an initial periapsis altitude of 300 km.

After Mars insertion, the aerobraking phase starts with a series of walk-in maneuvers. The strategy is to gradually bring the periapsis altitude down to a level such that the dynamic pressure and heating rate satisfy pre-set corridor conditions for aerobraking main phase. While the periapsis altitude is within the upper bound of the Martian atmosphere, the spacecraft will be experiencing deceleration induced by atmospheric drag. In about six months, the orbit period will be reduced to about 2 hours from a 35-hour initial orbit period. The total energy saving is equivalent to about 1200 m/s in ΔV.

To maintain an allowable dynamic pressure corridor, the periapsis altitude is controlled via aerobraking maneuver (ABM) implementation. Typically, the ABMs are executed at apoapsis to either raise or lower the

periapsis altitude. JPL has successfully adapted the proven techniques in several inner-planet orbiters including previous Venus[4] and Mars[5,6] missions.

To accommodate spacecraft anomalies or ground outages (e.g. network, power, etc.), MRO is required to maintain a 48-hour orbit lifetime. Aerobraking will transit to the walk-out sub-phase as the lifetime constraint is encountered. Analysis shows that MRO periapsis altitude will be steadily increased at this time due to the Mars oblateness effect. Unlike previous missions, ABMs were used to raise the periapsis altitude to satisfy the lifetime requirement. In contrast, MRO is likely to use the periapsis-down maneuver to maintain a proper corridor and continue aerobraking without violating the constraint. When apoapsis altitude reaches 450 km, an aerobraking termination maneuver (ABX) will be performed to raise the periapsis altitude out of atmospheric influence. This event will occur sometime around September 2006. Figure 2 shows the concept of aerobraking and the drag-pass spacecraft attitude.

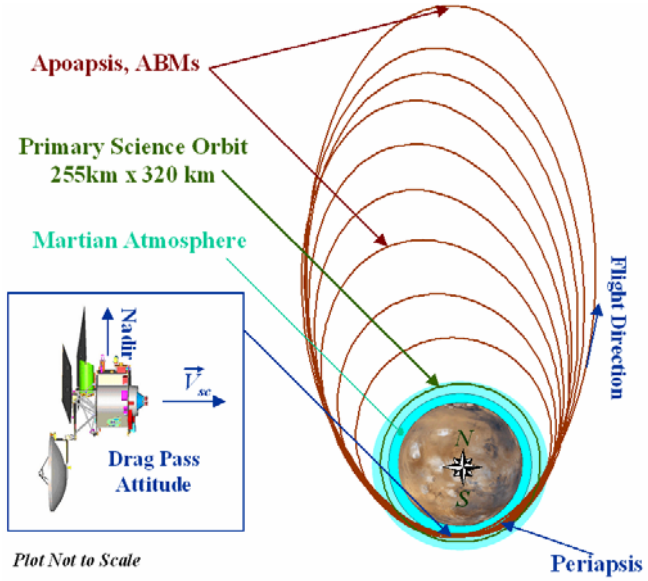

Figure 2: Aerobraking Illustration

Following the completion of ABX, MRO will settle in a 275 km x 450 km temporary orbit, marking the exit of the walk-out sub-phase. A transition-to-primary-science sub-phase will take place and can last from one to three months depending on the aerobraking conditions. Two orbit adjustment maneuvers (OA) and one inclination adjustment maneuver are scheduled during the first two weeks to establish a 255 km x 320 km primary science orbit (PSO). Prior to solar conjunction, occurring during the last four weeks of transition sub-phase, the on-board instruments will be deployed and calibrated. Navigation will start to characterize the uncharted dynamic regions, such as local variations of the Martian atmosphere and gravity. This first-hand experience will be applied to enhance the navigation dynamic modeling for supporting the primary science phase.

MRO primary science phase (PSP) will begin its one Mars-year investigations once the solar conjunction ends in early November 2006. A frozen orbit is designed to satisfy the science objectives. With local mean solar time fixed at about 3 pm and argument of periapsis at the South Pole, orbit trim maneuvers (OTMs) are planned regularly to maintain the Sun synchronized orbit. During this phase, MRO is expected to bring back 34 Terabits of data volume. It is equivalent to 28.9 billion pages of plain text, exceeding combination of all previous interplanetary missions.

After completion of the mapping and science investigations on the red planet, MRO will transit to relay phase for the next two years. Utilizing the on-board Electra system, MRO will serve as a relay station for the incoming spacecraft or ground assets. It can serve as a communication satellite for data relay and/or also as a space tracking station for navigation support. Future missions of the Mars Exploration Program such as Phoenix and Mars Science Laboratory (MSL) are candidates for this service. The MRO nominal mission will end December 2010 and the orbiter will be raised above the atmosphere for energy conservation.

B. Key Navigation Requirements

During launch phase, Navigation's major responsibility is to provide trajectories or separation states for supporting initial acquisition and critical events monitoring. Continuous navigation support is critical through launch plus 12 hours. The orbit information updates in the first several hours require fast turn-around solutions. The updated knowledge is to support the ground-station handover or acquisition of the subsequent stations.

MRO project requires Navigation placing the Mars capture orbit within 50 km of the targeted altitude, 300km. Further, without executing additional maneuvers, Navigation also needs to ensure that the post-MOI periapsis altitude is bounded within 200-400 km for the next eight consecutive orbits. These are the driving elements that determine orbit estimation and TCM/MOI strategy. Once aerobraking begins, Navigation needs to predict the time of aerobraking periapsis passage to less than 225 seconds for each drag pass. This is to guarantee that there is enough timing margin to configure and orient the spacecraft to an aerobraking-ready mode before entering the drag pass. In operation, the actual guard-band is slightly larger than 225 seconds.

Navigation is required to meet long-term and short-term prediction requirements in the primary science phase. The long-term orbit ephemeris needs to be known well enough to select the observations such that the predicted off-nadir pointing will not exceed more than 3 degrees 28 days from orbit determination data cutoff. The 3-degree uncertainty is equivalent to about 195 km of downtrack error or 59 seconds of timing error at the equator. The short-term prediction needs to satisfy 1.5 km of downtrack accuracy. It is about 0.5 seconds in terms of timing uncertainty. To meet these requirements during science operations, navigation of MRO, unlike previous missions, must account for drag from the highly versatile atmosphere, the dominant error source for ephemeris prediction. To minimize the modeling errors of the non-gravitational forces such as atmosphere drag and solar radiation pressure, Navigation also needs to have the capability to receive, process, and generate the quaternion data file and small force file to satisfy the spacecraft dynamic models for orbit determination. Table 1 summarizes the navigation PSP requirements.

Table 1: Navigation PSP Requirement Summary

	Position (km) - 3σ		
	Downtrack	**Radius**	**Crosstrack**
Long-Term Predict	195 (3 deg)	NA	1.00
Short-Term Predict	1.50	0.04	0.05
Reconstruction	0.10	0.015	0.04

III. Key Spacecraft Systems and Dynamic Models

Accurate spacecraft modeling is vital for precision navigation. Modeling of the sophisticated spacecraft dynamics is a primary challenge for MRO Navigation. The uncertainties in modeling the non-gravitational forces including:

1. Solar radiation pressure acts on the irregular-shaped spacecraft bus, and gimbal-enabled solar array and high gain antenna;
2. Thruster firings occur for the momentum buildup desaturation, attitude control, or any unexpected anomalies;
3. Any unanticipated outgassing may encounter;
4. Propulsive maneuvers are implemented for trajectory/orbit control; and
5. Martian atmosphere drag is experienced at low orbit altitude.

Prior to the aerobraking phase, mis-modeling of the solar radiation pressure and thruster events are the dominant error sources. To improve the modeling accuracy, in addition to passive fine-tuning, two active calibrations are planned in early cruise and approach phases. In primary science phase, with its low orbit altitude, atmosphere drag becomes a significant factor contributing to the orbit determination error. To make things even more challenging, the complexity of the spacecraft attitude control strategy and science operation further complicates the efforts of removing the unwanted error contributions. Several measurable efforts have been undertaken to enhance the modeling functions, one being navigation software updates. Examples include improving computation of the effective area of the spacecraft components, incorporating the detailed knowledge of the attitude changes, and developing additional capability of the Mars Global Reference Atmosphere Model (MarsGRAM).

To model the spacecraft dynamics and observations, Jet Propulsion Laboratory's (JPL's) Double Precision Trajectory (DPTRAJ) and Orbit Determination Program (ODP) are used for the computations. The trajectory is expressed in the J2000 Solar System Barycentric Reference frame. Currently JPL's DE405 is the source of the planetary masses and ephemeris. The position uncertainty of Mars in DE405[7] is about 6 km. A more recent ephemeris, DE410[8], is available for future upgrade and the associated Mars position uncertainty is less than 1 km, a significant improvement over the DE405 especially along the Mars out-of-plane component.

A. Spacecraft Systems

MRO consists of one structure subsystem (bus) and three main mechanisms (gimbals). Shown in Fig. 3, the skeleton of the bus supports all the science instruments and engineering subsystems such as telecommunications, propulsion, command and data handling, guidance navigation and control, electrical power, and thermal systems.

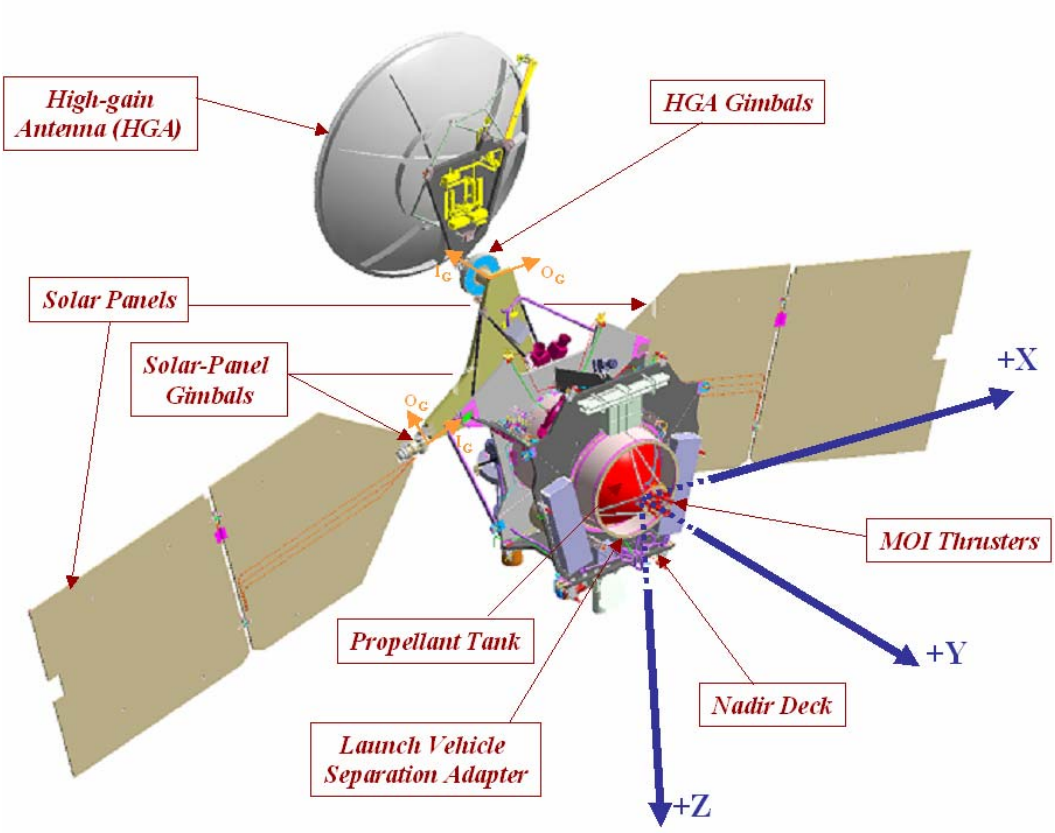

Figure 3: MRO Spacecraft

The gimbals, two each for the solar arrays (SA) and high gain antenna (HGA), have the capability of performing two-degree-of-freedom articulations. Each set of gimbals includes one inner gimbal and one outer gimbal motors to perform independent orientations.

MRO utilizes a three-axis stabilized Attitude Control System (ACS) that primarily relies on the Star Trackers, Sun Sensors, Inertial Measurement Unit (IMU), and Reaction Wheel Assembly (RWA) for attitude control. The spacecraft attitude measurements are provided via star trackers and Sun Sensors. In between the measurements, it

Table 2: Thruster Types and Specification

Specification	Thrust (Newton)	Number of Thrusters	Use
MR-107N	170	6	Main Engine Thruster: Use for TCM1 and MOI Maneuver
MR-106E	22	6	TCM Thruster: TCMs, MOI thrust vector control, OTM, ABM
MR-103D	0.9	8	ACS Thruster: ACS, AMD

depends on the IMU for attitude estimation and propagation. The knowledge (i.e. on-board reconstructed) of the attitude information will be temporarily stored onboard and played back through the engineering telemetry channels to the Ground Data System (GDS)[9] when DSN communication is available. With the on-board reconstructed attitude information, the navigation team is able to model the spacecraft orientation much more accurately. The information is expressed in terms of quaternion representations and component gimbal angles.

The propulsion system operates in a blow-down mode for all thruster events except MOI burn where a pressure regulator will be used to improve the burn efficiency. A monopropellant system is used to reduce the complexity of the propellant management. As more and more hydrazine is used during cruise and approach phases, the tank pressure will drop to about 160 psi after TCM5 from its peak 205 psi. To maintain a reliable thruster operation, a minimum of 100-psi tank pressure is necessary.

There are three types of the thrusters used in the operation. Table 2 summarizes their usages and configuration. The main engine thrusters are specifically designed for MOI burn. To minimize the risk of first-time use of these powerful 170-Newton thrusters during orbit insertion, TCM1 will be executed via the Main Engine as part of the risk reduction management.

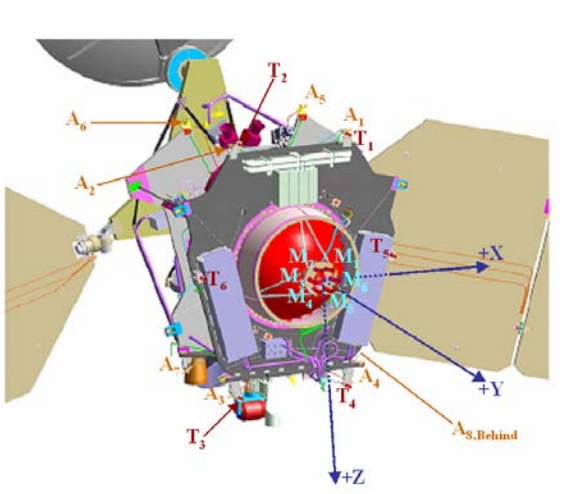

Figure 4: Thrusters Locations

Besides use on the flight path control, TCM thrusters are also employed to perform MOI thrust vector control. Figure 4 shows the locations of the thrusters. A_1 through A_8 are the ACS thrusters, T_1 through T_6 are the TCM thrusters, and M_1 through M_6 are the Main Engine thrusters.

In addition to performing the Angular Momentum Desaturations (AMD), the ACS thrusters are also used on maintaining the aerobraking drag attitude. Arranged in couples, the ACS thrusters are fired in pairs, so that the resulting net ΔV is 0. Although it is designed as a balanced thruster system, a small amount of the residual ΔV for each thruster activity is anticipated in operation.

MRO relies on the X-band radio system communicating with the Earth. The on-board antenna system includes a 3-meter diameter High Gain Antenna, and two Low Gain Antennas (LGA). Although the LGAs have the capability of transmitting and receiving data, Navigation primarily depends on the HGA to obtain the radio-metric tracking data. The small deep space transponder (SDST) is capable of supporting two-way and one-way radio operations. It either gets the reference frequency from an uplink signal source for a two-way link or obtains the reference frequency from the on-board Ultra Stable Oscillator (USO) or the built-in auxiliary oscillator (AUX/OS) for a one-way link. In addition to the conventional tracking data capability, the SDST also can generate the Delta-DOR (DDOR) tone for VLBI observations.

B. Spacecraft Coordinate System and Orientation

As illustrated in Fig. 3, the perpendicular spacecraft body fixed coordinate system is defined such that +Z is along the normal direction of the nadir deck, +Y is along the center line of propellant tank and MOI thrusters, and +X is determined by the right-hand rule (i.e. cross product of +Y and +Z). The origin of the coordinates is located at the geometric center of the Launch Vehicle Separation Adapter plate (i.e. at the end point of the propellant tank along the center line of the MOI-thruster module).

To model the non-gravitational accelerations due to the atmospheric drag and solar radiation pressure, the physical structure of MRO is decomposed into nine representative components. These include a 3-meter diameter circular HGA plate, two 12-m^2 two-sided solar-array flat plates, and six 7-m^2 one-sided flat plates for the spacecraft bus. At zero-degree gimbal angles (both inner and outer gimbals), the normal directions of the cell-side panels are along –Y axis and the geometric long sides of the panels are along the ±X axes with each panel canted 15-degree toward +Z axis. Both sets of the solar-array gimbals are capable of rotating along I_G (inner gimbal rotation axis) and O_G (outer gimbal rotation axis) to track the Sun. However, during cruise and aerobraking, the solar-array configuration is to set gimbal positions to zero degrees. Similar to the solar array, the HGA gimbals also provide a two-axis rotation capability maintaining the Spacecraft-Earth communication. Illustration of the gimbal rotation axes (i.e. I_G and O_G) is shown in Fig. 3 (the directions denote positive rotations). The gimbal locations are fixed relative to the spacecraft mechanical frame.

After the orbiter is separated from the launch vehicle, through a series of appendage-deployment activities, MRO will be settled in a preset inertial-fixed initial acquisition attitude. The orbiter +X is determined by the cross product of Sun and V_{inf}, –Y axis is pointed to the Sun with a bias of 15-degree rotation about –X axis, and the gimbal positions of solar arrays and HGA, (I_θ,O_θ), are (0,0) and (180,–45) degrees, respectively.

Depending on the status of spacecraft system checkout and the condition of the appendage deployment, at approximately launch plus 3 days, MRO will transit from the initial acquisition attitude to the Sun-point cruise attitude. The attitude is in a configuration such that the spacecraft –Y axis tracks the Sun, –X axis is determined by the cross product of the Sun and Earth, the solar gimbal angles, (I_θ,O_θ), are set to (0,0), the HGA inner gimbal angle, I_θ, is fixed at 180 degrees, and the HGA outer gimbal, O_θ, is the result of the Sun-Probe-Earth angle, Φ_{SPE}, subtracting 90 degrees. This ensures the Earth always lies on the –YZ plane. In this configuration, the HGA can easily track the Sun via the outer gimbal rotation and maintain the inner gimbal angle constant. Figure 5 demonstrates the Sun-point cruise attitude.

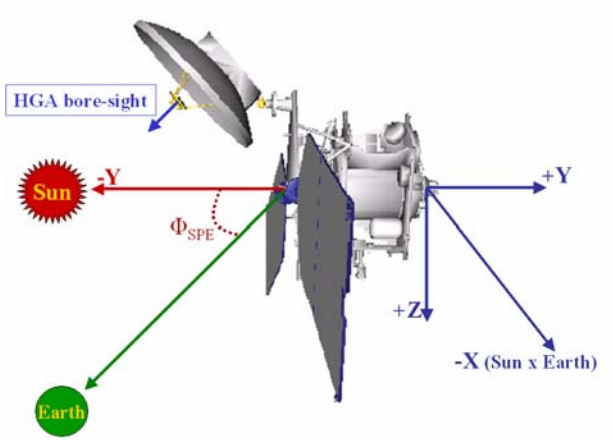

Figure 5: MRO Cruise Attitude

Two months prior to the Mars Orbit Insertion, the spacecraft will be articulated to a "spread-eagle" configuration. Figure 3 illustrates the spacecraft in a "spread eagle" configuration. Both of the solar-array gimbal positions, (I_θ,O_θ), are set to (0,0) degrees. The HGA inner gimbal angle, I_θ, and outer gimbal angle, O_θ, are fixed at 180 degrees and –90 degrees respectively. The nominal spacecraft attitude in this phase is defined as: –Y axis is pointed to the Earth (i.e. HGA point to the Earth), the pointing direction of +Z is the vector-cross product of Earth x Sun, and +X is determined by +Y x +Z.

Not only is the "spread eagle" configuration used in approach and MOI phase but also in aerobraking phase, TCMs, and AMD desaturation. Two distinct attitudes are designed specifically for aerobraking:

1. Vacuum Attitude: Use when the orbiter is in vacuum space. HGA bore-sight (i.e. –Y axis) points to the Earth, +X axis is obtained by Earth x Sun, and Z is determined by right-hand rule.
2. Drag-pass Attitude: Use when the orbiter is in drag pass. The spacecraft +Y axis is along the velocity vector, +X axis is along the orbit angular momentum direction, and Z is determined by right-hand rule.

Once the orbit is established for science operation, MRO will be configured in nadir and/or off-nadir attitudes. The nadir attitude is defined such that the nadir deck (or +Z axis) points directly on Mars, +X axis is along the velocity vector, and +Y axis is determined by the right-hand rule. The solar-array and HGA gimbals are articulated to track the Sun and Earth. To compensate the navigation prediction error and increase the site-revisit opportunity, MRO is capable of performing off-nadir targeting that enables the spacecraft to roll about +X axis with maximum 30 degrees of roll angle. Compared with the nadir attitude, the off-nadir pointing is constrained due to telecom and power limitations. For instance, the maximum number of off-nadir rolls per orbit is limited to 4, negative roll (i.e. –X) can not exceed two per orbit, maximum roll angle is constrained at certain time span (due to gimbal singularity and power constraint), … and so on. In addition to the nadir and off-nadir attitudes, MRO constantly applies a small yaw (about +Z axis) and pitch (about +Y axis) to adjust the pointing misalignment due to the Mars rotation. Also, when performing a hi-stability imaging session, the solar-array gimbals are required to freeze to prevent any vibration induced by the spacecraft motion.

C. Solar Radiation pressure

A simplified form, shown in Eq. (1), is used to describe the total solar radiation force experienced by the spacecraft:

$$F_{solar} = \left(\frac{C_{sf} S_{solar}}{R_{sp}^2} \right) \left(\sum_{i=1}^{9} A_i f_i(\mu_i, \nu_i, \psi_i, \ldots) \right) \tag{1}$$

As described in previous sections, the spacecraft is modeled as a 9-component structure. The orientation of each individual component with respect to the orbiter is defined either by gimbal articulations or fixed relative to the spacecraft mechanical frame. Additionally, query of the spacecraft attitude information (as discussed in Section III-B) is available via either telemetry channel (reconstruction) or prediction generator. The effective area for each component, A_i, then can be computed through the knowledge of spacecraft gimbal and attitude information. In Eq. (1), the DPTRAJ inputs, μ_i and ν_i, are formulated from the following equations[10,11]:

$$\mu_i = \frac{1}{2}\beta_i\gamma_i \tag{2}$$

$$\nu_i = \frac{1}{3}\left[\gamma_i(1-\beta_i) + \kappa_i(1-\gamma_i)\right] \tag{3}$$

The spacecraft team will provide the surface properties β_i, γ_i, and κ_i pre-launch. The effective area and reflectivity coefficients in Eq. (1) will be reconstructed via the orbit determination process. In conjunction with the solar pressure calibration, these parameters will be updated during cruise.

D. Mars Atmosphere Model

Unlike previous missions to Mars, MRO will spend its entire science collection period at altitudes where the atmosphere has a noticeable effect on the trajectory. For this reason, special emphasis has been placed on modeling the Martian atmosphere. The basic model currently in use is the Mars Global Reference Atmosphere Model (MarsGRAM)[12]. The latest version of MarsGRAM (version 2001) uses as its inputs tables of various atmospheric parameters output by the NASA Ames Mars General Circulation Model (MGCM) and the University of Arizona Mars Thermospheric General Circulation Model (MTGCM). These models are physically based and cover the entire planet. MGCM provides data tables below 80 km altitude; MTGCM provides the tables between 80 and 170 km altitude. Above 170 km, MarsGRAM 2001 uses information from a modified Stewart thermospheric model. The code interpolates between the models to make a smooth transition between MTGCM and the Stewart models between 155 and 170 km. Altitude values can be computed either above a reference ellipsoid or the more detailed areoid measured by the Mars Orbiter Laser Altimeter (MOLA). Another update to the atmosphere model is anticipated in January 2005. Key updates include traveling wave model, new database of MGCM and MTGCM, and options for the input parameters. Prior to the final tweak, a beta version will be released in Oct 2004 for test. Figure 6 shows the data structure of MarsGRAM.

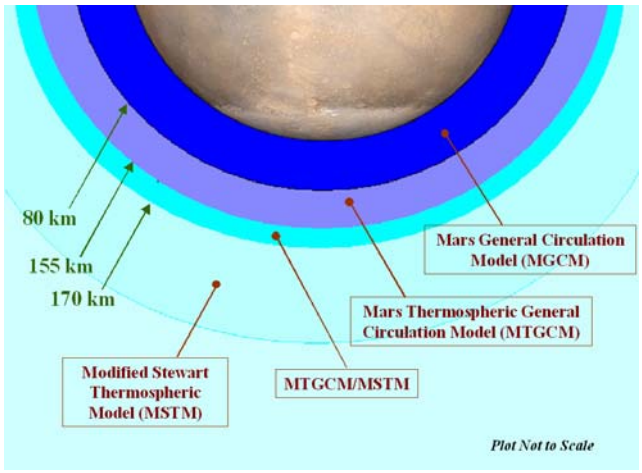

Figure 6: MasGRAM Atmospheric Data Structure

Equation (4) formulates the DPTRAJ atmosphere drag model:

$$F_{atm} = \left(\frac{\rho_{atm} V_{sc}^2}{2}\right) C_D \left(\sum_{i=1}^{9} \tilde{A}_i\right) \vec{V}_{sc} \tag{4}$$

The density (ρ_{atm}) is interpolated from the MarsGRAM model, and the component effective drag areas ($\tilde{A}_i$) are computed by using the spacecraft attitude information. The spacecraft team provides the overall drag coefficient (C_D) in development phase.

As described in Section III-B, during primary science phase, the spacecraft orientation is complicated by the gimbal articulation. Furthermore, the off-nadir targeting increases the uncertainty in modeling the spacecraft orientation. With both of the solar panels continuously tracking the Sun and the bus +Z axis pointing at nadir direction, it resembles the hovering of a slow-motion hummingbird. One of the major challenges is that the computation of drag effective areas must consider the appendage articulations in the dynamic modeling, or there will be a noticeable orbit error either in the estimation process or trajectory propagations. Another challenge in the drag modeling is the spacecraft self-shadowing effect induced by the gimbal motions. Viewed from the drag direction, the Sun-tracking motions of the solar panels create different levels of bus shadowing effects. Figure 7 illustrates the spacecraft self-shadowing configuration. As seen from the figure, the X-side bus is entirely shadowed by one of the solar panels. It almost accounts one-third of the total effective drag area. Since the orbit is frozen at 3 pm and the X-side bus nominally is along the drag direction, this causes the shadowing factors to vary up to 30% in an orbit. This implies the mis-modeling is not a constant bias and cannot be easily taken out. If it includes an average of 3 off-nadir targets per orbit (roughly 15-20 minutes per off-nadir session), it will further increase the difficulty of the drag modeling. In addition, modeling of the total effective area in solar radiation pressure has a similar concern. However, compared with the level of drag acceleration during the PSP, the error is relatively small. Although the current software capability does not take into account the self-shadowing effect and gimbal articulation, software updates are in progress to enhance the modeling functions.

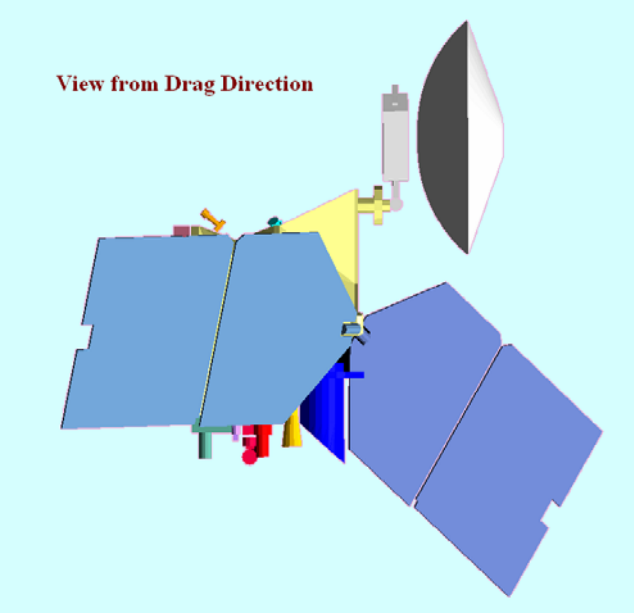

Figure 7: Spacecraft self-shadowing during PSP

E. Mars Gravity Model and Small Forces

Currently MRO is using MGS85F2 gravity field for analysis and reference trajectory computations. This is a spherical harmonic expansion complete to degree and order 85. Due to its enormous size, it is impractical to use the full covariance for error studies. A subset of the covariance using the Spectrum of Linear Orbit Perturbations (SLOP)[13] method is adapted for the covariance analysis. MGS85F2 gravity model is based on the IAU 2000 Mars pole and prime meridian locations and a reference radius of 3396.2 km, consistent with the mean equatorial radius measured by the MGS laser altimeter. The MGS85F2 field was developed at JPL using data collected from Mariner 9, Viking 1 and 2, and MGS mapping through Nov. 18, 2001. Prior to launch, an updated version will be used for operation.

Navigation anticipates some degrees of local gravity variations because of low science-orbit altitude. To account for the perturbation, estimation of the local gravity may be necessary early in the primary science phase until an improved version is available.

Although the reaction wheel assembly usually performs the spacecraft orientation changes, there will be time when the Attitude Control System uses its balanced thrusters for attitude control/maintenance and momentum desaturation. The small force file will be used to model any resulting net ΔV from the thruster activities.

F. Calibrations

1. Thruster Calibration

The thrusters are coupled by design so in theory, no net translational ΔV is expected to be imparted to the spacecraft. However, since the thrusters cannot be mounted and oriented perfectly, it is realistic to expect a net translational ΔV. In order to be able to predict the motion of the spacecraft, especially in the Primary Science Phase, well enough to meet prediction requirements, it is necessary to calibrate this ΔV. This will be done by performing a thruster calibration activity early in the cruise phase of the mission. This calibration will involve slewing the

spacecraft to three mutually orthogonal attitudes, where typical AMD-type burns will be forced upon the spacecraft and the resultant ΔV will be measured. The orientation choice is made fairly simple by pointing each of the three spacecraft fixed axes (X, Y, Z in Fig. 3) of the spacecraft towards the Earth.

For each of the three attitudes, there will be six types of burns: ±yaw (rotation about ±Z), ±pitch (rotation about ±Y), and ±roll (rotation about ±X). The RWA wheels will be spun up and down in order to produce a positive and negative desaturation of each axis. Since the net ΔV vector is three-dimensional, three orthogonal attitudes are required in order to reconstruct it. The desaturation logic to be used in the thruster calibration will be the same as that for a typical AMD. This implies that the thruster pulse-width will be fixed at 0.4 seconds per pulse and the time between pulses will be fixed at 10 seconds. 50 to 100 pulses will be required for each AMD (a total of 18 will be performed: six per each of the three attitudes).

The effect of the AMD on the spacecraft is only one of several perturbing forces that the orbiter will experience. Therefore, in order to assist the navigation team in being able to distinguish this effect from that of other sources, namely solar radiation pressure, there will be a quiescent time between each burn and attitude change. The expected quiescent time should be no less than approximately 10 minutes. This brings the total thruster calibration activity time to approximately nine hours.

Via the Low Gain Antenna (LGA), high-rate Doppler data is expected throughout the thruster calibration activities. RWA wheel speed, obtained in normal telemetry, will be used as an independent source of force reconstruction to be compared against the results obtained from the Doppler data. The other data type used in the reconstruction of the burns is the small force telemetry, which will also be collected and played back. Thus, the calibration event will serve the dual purpose of both determining the residual ΔV and validating the onboard computation of the small force events.

2. Solar Pressure Calibration

The purpose of solar radiation calibration is to verify the overall solar pressure model and refine the solar reflectivity coefficients. Two-way Doppler and range data are used to estimate directly for the s/c accelerations experienced as an effect of the SRP environment (non-line-of-sight contribution not visible). Similar to the thruster calibration, the RWA data can also be used for independent check. Continuous tracking and a 7-day quiescent period are required to ensure the success of this activity. In order to better determine the out-of-plane accelerations, DDOR data are highly desired pre and post-calibration.

Due to the simplified model and to inaccuracies in computing surface properties, it is difficult to exactly model the dynamic effects of solar radiation pressure prior to launch. Therefore, during cruise, one 7-day time slot (around the beginning of the approach-MOI phase) will be allocated to calibrate the model. In order to capture the desired quantities as best as possible, it would be ideal that the spacecraft not experience non-gravitational forces other than that caused solely by the SRP. This implies that thrusting events, like those used for AMDs, are minimized during the SRP calibration activity. Maximum quiescent periods at specific attitudes are desired. An AMD is forced prior to the calibration activity, and attitude changes are to occur on RWA control authority. It will not be possible to separate the reflective properties of all of the spacecraft surfaces due to physical constraints in possible spacecraft configurations. However, it should be possible to characterize the combined contribution of the various surfaces to the solar radiation pressure environment. Finally, to separate the contribution of the diffuse component of SRP (which acts along the surface normal) from the specular component (which acts both parallel and normal to the surface), it is desired to have the areas at Sun off-pointing angles of greater than 45 degrees.

IV. Tracking Data and Filter Strategy

A. Navigation Tracking Data

Two-way X-band Doppler is the main data type that will be used during all mission phases. The Doppler observables from the DSN tracking sites are modeled using the differenced range formulation in the DPODP. The transformation of the location of the tracking station from body fixed to inertial coordinates includes polar motion calibrations and UT1-TAI timing corrections, solid Earth tides, and Earth center of mass correction. In addition to the seasonal corrections, the diurnal troposphere and ionosphere calibrations are also included in the computation. The Earth Orientation Parameter (EOP) data file is the source of the polar motion and timing corrections. Additionally two-way range and Delta Differential One-way Range (ΔDOR) are used regularly during cruise phase and occasionally during primary science phase. Table 3 summarizes navigation tracking data during each mission phase. Although the Ka-band data is not part of baseline tracking plan, it is included for reference.

Table 3: Navigation Tracking Data Summary

Mission Phase	Key Events	Begin	End	Doppler	Range	DDOR	Remark
Launch		L+000d	L+030d	Continuous	Continuous		
	TCM1	L+015d		Continuous	Continuous		Dual Track
Cruise		L+030d	M-060d	1p/day, X 1p/wk, Ka	1p/day, X 1p/wk, Ka	L+040d to M-060d: 1/wk, X TBD, Ka	8 hrs/pass for F2/SRA
	TCM2	L+090d		Continuous	Continuous		±3days, Dual Track
Approach & MOI		M-060d	M+007d	Continuous, X 1p/wk, Ka	Continuous, X 1p/wk, Ka	M-060d to M-40d: 1/wk, X TBD, Ka	
						M-040d to M-005d: 2/wk, X TBD, Ka	
	TCM3	M-040d		Continuous, X	Continuous, X		Dual Track
	TCM4	M-010d		Continuous, X	Continuous, X		Dual Track
	TCM5ab	M-001d	M-006h	Continuous, X	Continuous, X		Dual Track
	MOI	M+000d		Continuous, X	Continuous, X		Dual Track
Aerobraking (AB)		M+007d	M+242d				
	AB	M+007d	M+189d	Continuous, X	Continuous, X		8 hrs/pass
	Transition	M+189d	M+242d	2p/day, X	2p/day, X		8 hrs/pass
	Solar Conj.	M+213d	M+242d	1p/day, X	1p/day, X		8 hrs/pass
Primary Science Phase (PSP)		M+243d	M+984d	2p/day, X 2p/wk, Ka	1hr/day		
	Science Augmnt.	M+243d M+826d	M+560d M+984d	3p/wk, X			70-meter Antenna; 8 hrs/pass
	Solar Conj.	M+985d	M+1019	1p/day, X, Ka	1hr/day		
Relay		M+1020	M+1757	1p/day, X, Ka	1hr/day		

B. Estimation and Maneuver Strategy

Navigation operation strategy is based on the covariance analyses, maneuver analysis, and dynamic sensitivity studies. Creating a simple and efficient estimation strategy is Navigation's top priority; however, to satisfy the navigation accuracy requirements, variants of the standard filter strategy are developed for different mission phases. The variations are mainly due to the trajectory/orbit conditions and spacecraft dynamic environment changes such as gravity, atmosphere, spacecraft attitude, and thruster activities.

Table 4: Maneuver Epochs

Maneuver		Epoch	Purpose
TCM 1		Launch + 15 days	Correct injection errors, remove injection bias, and target to final aimpoint
TCM 2		Launch + 90 days	Correct for OD and maneuver execution errors
TCM 3		MOI - 40 days	Correct for OD and maneuver execution errors
TCM 4		MOI - 10 days	Correct for OD and maneuver execution errors
TCM 5	**A**	MOI – 24hrs	Orbiter Safety only; no statistical components
	B	MOI-6hrs	

During cruise and approach-MOI phases, there are five trajectory correction maneuvers, TCM1-5, planned to best condition the trajectory for Mars insertion. TCM1 is designed specifically to remove the targeting bias and orbiter injection error. The targeting bias is introduced in the design to satisfy the probability of impact requirement and reduce the risk of first-time use of the main engine (see section III-A). Except TCM5 is served as a contingency maneuver, TCM2-4 is

designed to correct the trajectory error induced by navigation uncertainties. TCM5 is an off-the-shelf maneuver with two execution opportunities at MOI-24 hours and MOI-6 hours (TCM5A and TCM5B). They both are pre-designed to solely raise the encounter altitude to a safe distant in case of trajectory error.

The relative timing of the cruise maneuvers takes into account the dynamical capability to change the Mars encounter at various times. The Type-I interplanetary trajectories for MRO do not show transfer-angle constraints or other singularities, and so the TCM timing is based primarily on operational considerations and standard practice. The TCM epochs for cruise are shown in Table 4. The relative timing of the TCMs does not change throughout the launch period.

Table 5 summarizes the maneuver execution error requirements. The knowledge is used as *a priori* assumptions for orbit determination, covariance studies and maneuver analyses, and statistical mapping. Table 6 shows the standard data weight (one sigma). During solar conjunction periods, two-way Doppler will be significantly de-weighted because of the solar plasma influence. The level of degradation depends on the solar activity and the Sun-Earth-Probe angle. Typically, if the Sun-Earth-Probe angle is less than 3 degrees, the tracking data is unusable for navigation purpose.

Table 5: Maneuver Execution Error Requirements (3σ)

Error Source	Error
Fixed Magnitude	0.02 m/s
Proportional Magnitude	2%
Proportional Magnitude (MOI only)	1%
Fixed Pointing (per axis)	0.02 m/s
Prior to PSP, Proportional Pointing (total)	2% ($\Delta V > 10$ m/s)
	4% ($\Delta V \leq 10$ m/s)
PSP and later, Proportional Pointing (total)	2% (All ΔV)

Table 6: Data Weight (1σ)

Data Type (X-Band)	Data weights	Remark
2-way Doppler	0.1 mm/s	60 Second Sampling
2-way range	4 m	
Delta DOR	4.5 nrad	0.12 ns

Standard estimated filter assumptions are summarized in Table 7. The estimated parameters are divided in two categories: constant and stochastic parameters. Constant parameters are estimated to take out any systematic biases induced by the modeling errors. If the mis-models are random and unpredictable, a stochastic noise model is included in the estimation process. Currently, the random noise is modeled as a piecewise constant with the input options of either the first-order exponential model or random-walk model. MRO Navigation mostly uses the first-order exponential model (also known as first-order Markov model) for the random parameters that the process noise is bounded by a steady state sigma. Equation (5) describes a discrete system[14] of the color (correlated) noise model:

$$\sigma_{j+1}^2 = \sigma_j^2 m_j^2 + (1 - m_j^2)\sigma_{ss}^2 \tag{5}$$

The process noise of the next batch, σ_{j+1}, is correlated with the current σ_j by the exponential correlation function, m_j, current batch process noise, σ_j, and steady state sigma σ_{ss}. A special case of the color noise can be derived from Eq. (5). Setting the exponential correlation function, mj, to zero, the process becomes uncorrelated. Often this is referred to as a white noise stochastic process.

Table 7: Estimated Parameters (1σ)

Estimated Parameters	Estimate Type	*A priori* uncertainty (1σ)	Remark
Position	-	100,000 km	All Phases
Velocity	-	10 km/s	All Phases
Angular Momentum Desaturations	Constant Bias	0.133 mm/s	Cruise and PSP: every 48 hrs, spherical
Gravity	Constant Bias	3x MGS85f2 fields	PSP
OTM	Constant Bias	•Proportional: 0.67% •Fixed: 0.67 cm/s	PSP: Based on 0.8 m/s magnitude burn, applied spherically. 1st occurs in data arc, 1 day before DCO, 2nd occurs 27 days after DCO.
Solar Pressure (Scale Factor)	Constant Bias	10%	All Phases
Solar Pressure Mis-modeling	Stochastic	3.6 x 10^{-12} km/s^2	Cruise: white noise
Outgassing	Stochastic	Vary	Cruise: Random walk stochastic, with steady state sigma following curve
	Bias	2x10^{-13} km/s^2	PSP, Aerobraking: Bias at 2x10^{-13} km/s^2 [E- aerobraking, PSP]
Atmospheric Drag (C_D)	Stochastic	35%	Aerobraking: white noise PSP: color noise
	Bias	25%	PSP: if not correlated

Table 8: Considered Parameters

Considered Parameters	Considered Type	*A priori* uncertainty (1σ)	Remark
Atmospheric Drag (Cd)	Bias	10% Bias	PSP: Starts 2 weeks into prediction
Gravity Field	Bias	3xMGS85f2 field	Aerobraking
Solar Pressure Coefficient (Scale Factor)	Bias	10% Bias	PSP
X, Y Pole Motion	Bias	10 cm	All Phases
UT1-UTC	Bias	10 cm	All Phases
Troposphere (wet)	Bias	4 cm	All Phases
Troposphere (dry)	Bias	1 cm	All Phases
Ionosphere (day)	Bias	65 cm	All Phases
Ionosphere (night)	Bias	15 cm	All Phases
Station Locations	Bias	Covariance	All Phases

Unlike aerobraking when the atmosphere error is modeled as a white noise stochastic parameter, a color noise model is used for PSP analysis. Although there is no clear indication that the mis-modeling of Martian atmosphere is correlated at the science orbit, however, by examining the limited MGS and ODY atmosphere data, Navigation is able to find some local correlation. Typically, aerobraking only needs a 24-hour propagation while PSP needs to cover up to 8 weeks of prediction. In such a long predict, the correlation will be a significant error source.

Other than estimated parameters, there are also parameters that account for the modeling insufficiency that need to be considered in the covariance analysis. Table 8 summarizes the considered parameters.

V. Navigation Analysis

A. Navigation System and Process

Navigation adapts Multi-mission operation philosophy. The navigation processes and sub-systems have high level of heritage. Some of the key components have been established since the 1960's. Figure 8 illustrates the overall navigation data flow and system architecture. The Navigation System consists of several sub-systems including Double Precision Trajectory (DPTRAJ), Orbit Determination Program (ODP), Mission Analysis Software (MAS), Maneuver Operation Program Set (MOPS), Automated Radiometric Data Visualization and Real-time Correction X display (ARDVARC), Navigation Utilities, and Navigation Libraries. Each sub-system component

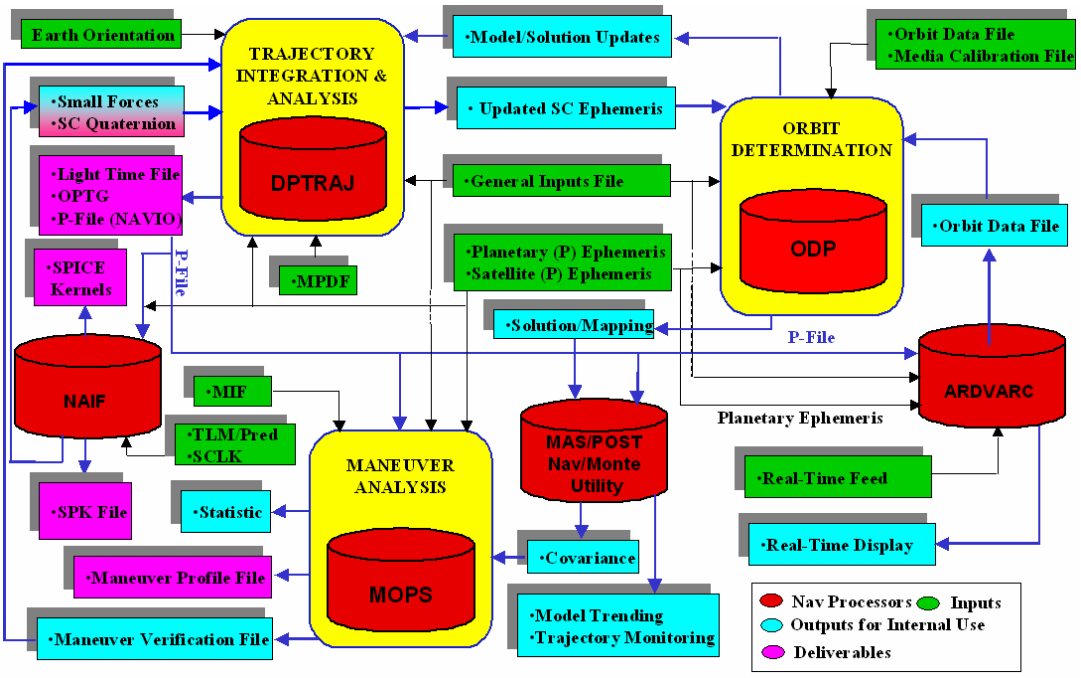

Figure 8: Navigation System Architecture and Data Flow

contains dozens of programs. As indicated in Fig. 8, the red represents the Navigation System processors. Green is the inputs from the other ground data systems. Blue represents products generated for internal usage. Navigation deliverables are shown as magenta.

The navigation process consists of several sub-processes. Orbit Determination (OD), Flight Path/Orbit Control and Trajectory Analysis, Spacecraft Dynamic (e.g. Thruster) Calibration, and Real-Time Spacecraft Event Monitoring are the major sub-system processes. Figure 9 illustrates a simplified navigation process. Trajectory Integration & Orbit Determination is one of the core sub-processes. It starts with a full range of information (data and models) collection. This includes receiving input files from ground data system, real-time engineering data system, and spacecraft engineering planning. The outputs then are used by other systems such as Science Planning and Sequence Development.

Additionally, the Flight Path/Orbit Control Analysis plays an important role in the process. It is responsible for the reference trajectory generation and maneuver design. The resulting design is incorporated in the spacecraft dynamic model. Integrated spacecraft ephemeris with maneuver(s) is used for trajectory analysis, planning, and product generations.

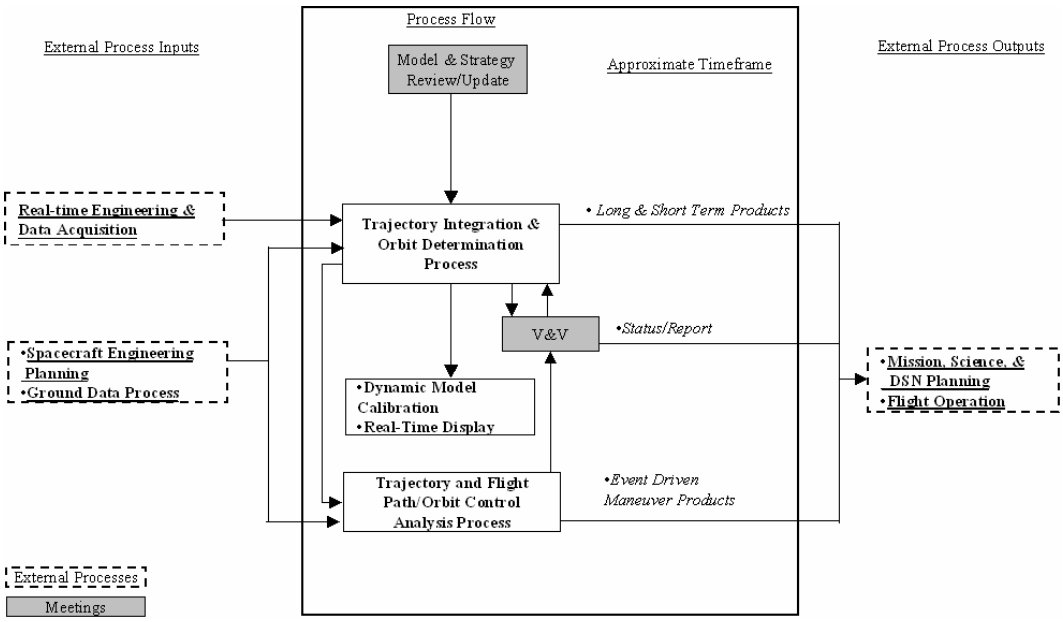

Figure 9: Navigation Process

B. Analysis Results

1. Cruise, Approach, and MOI

JPL's SIGMA program, a subset of DPODP, is used to perform the covariance analysis. Utility programs are used to simulate tracking data. TCM1 data arc is about 1 week, while the data arc is 30 days for TCM2-5. Tracking data is cutoff at 5 days prior to the execution of each TCM. The standard filter is used for error assumptions. Table 9 shows the OD and delivery B-plane mapping uncertainties in the Mars mean equator coordinate for the open launch period. The delivery statistic is the result of maneuver analysis using Monte-Carlo techniques, which include the effects of orbit determination uncertainty, injection errors, maneuver execution errors, and trajectory optimization inputs. The results are shown as the semi-major (SMA) and semi-minor (SMI) axes of the 3-σ uncertainty ellipse in the B-plane, the angle that the ellipse makes with respect to the T-axis (theta), and the Linearized Time-of-flight (LTOF), which is the along-track uncertainty. As indicated, the OD is the dominant error source of TCM1 and TCM2. Once the orbiter gets closer to Mars, the error distribution starts shifting from OD to

Table 9: 3σ Statistics at MOI

Maneuver		SMA (km)	SMI (km)	Theta (deg)	LTOF (sec)
Injection		290,580	19,392	-89.2	137,526
TCM 1	**OD**	4273	1779	68.3	2198
	Delivery	4671	1931	72.5	2417
TCM 2	**OD**	355	246.2	28.3	148.9
	Delivery	457.5	321.9	26.4	194.1
TCM 3	**OD**	93.3	75.3	1.0	22.0
	Delivery	140.5	116.7	-11.4	40.8
TCM 4	**OD**	22.1	16.8	59.5	4.7
	Delivery	33	30	57.4	10.6
TCM5	**A: OD**	9.3	2.8	124.8	0.6
	B: OD	9.9	1.0	127.8	0.2

maneuver. However, the domination is not obvious. Table 10 shows the TCM ΔV uncertainties for the 10 August'2005 launch opportunity.

The maneuver designs for MOI are presented in Table 11. The design is based on 3-σ low engine performance. Note that two designs are given for each arrival date. The "Optimal" design minimizes the velocity change by varying the maneuver pitch rate, start time and initial attitude. The incoming altitude at Mars is also varied to minimize the MOI delta-V. An option currently exists to design MOI to be fault-tolerant to a 14-minute interruption during the burn, achieving a safe orbit with a period of near-120 hours (or less) and a periapsis altitude above 250 km. This may be achieved by changing the start time of the MOI burn 2 minutes earlier. In this case the "Fault-Tolerant" design begins at this specified time and orbit altitude and changes the other free parameters (pitch rate and attitude) in order to minimize the MOI delta-V.

Table 10: Cruise ΔV Statistics

Maneuver	Mean DV (m/s)	1σ DV (m/s)	99% high (m/s)
TCM 1	4.4	2.6	12.1
TCM-2	0.18	0.12	0.53
TCM-3	0.06	0.03	0.14
TCM-4	0.06	0.03	0.13
Total Cruise	4.7	2.6	12.4

Table 11: MOI Maneuver Designs

Launch	Arrival	MOI Solution	DV (m/s)	Duration (sec)	Prop. (kg)	Pitch Rate (deg/s)	Incoming Altitude (km)
8/10/2005	**3/10/2006**	Optimal	1004.1	1638.7	786.8	0.023	384
		Fault-tolerant	1012.7	1649.8	792.2	0.026	NC
8/21/2005	**3/14/2006**	Optimal	914.6	1520.9	730.3	0.024	368
		Fault-tolerant	918	1525.5	732.5	0.022	NC
8/30/2005	**3/16/2006**	Optimal	887.1	1483.7	712.4	0.026	360
		Fault-tolerant	890.3	1488.1	714.5	0.024	NC

In addition to the delivery at MOI, the results at the capture orbit were also examined. Since the requirement was for the spacecraft to be in a safe orbit, with minimum periapse at 200 km and a maximum periapse at 400 km, for eight orbits past MOI, the TCM 4 delivery errors were mapped to eight orbits after MOI. Three parameters were examined: the periapse radius, inclination, and orbit period. The results were obtained by combining, in an RSS sense, several different error sources. The first was the OD delivery uncertainty at the TCM 4 cutoff, as shown in Table 9. This was combined with the pointing error for the MOI burn, taken as 2% of the nominal value of roughly 1 km/s, and the combination is assumed to cause errors which can be mapped linearly, that is, through the formal covariance mapped to the post-MOI orbit. Errors in the burn itself are of two varieties. The maneuver uses accelerometers to cutoff the thrust after the required ΔV is reached; the requirement on the accuracy is 1%, so the

Table 12: 3σ capture orbit uncertainties

	3σ OD + pointing	9% Overthrust (underthrust)	1% Overburn (Underburn)	RSS Total Overburn (Underburn)
Inclination (deg)	0.232	0.005 (0.019)	0.012 (0.011)	0.233 (0.233)
Period (hours)	1.09	1.15 (1.53)	2.38 (4.01)	2.85 (4.42)
Periapse Radius (km)	26.4	8.2 (16.7)	3.8 (1.5)	27.9 (31.3)

first error source is this uncertainty. The second error is on the magnitude of the nominal thrust provided by the six MOI thrusters, and the value used here was 9% of the nominal 170 N. Because of the pitch-over nature of MOI, neither of these error sources can be linearly mapped to post MOI. Thus, the procedure was to integrate a trajectory, individually varying the MOI ΔV and thrust magnitude by both positive and negative amounts with the values stated above. The changes in the orbital parameters are measured against those achieved with the nominal burn. The results are RSS'ed with the OD and burn direction errors. The results are shown in Table 12 for P9, the eighth orbit periapse after insertion. Only the degraded tracking case is shown. Note that the periapse radius uncertainty values are small enough such that spacecraft safety is not an issue assuming correct targeting to the MOI conditions and the nominal capture orbit is achieved. The orbit period uncertainties can be somewhat large, but should be taken care of in the aerobraking phase.

2. *Aerobraking*

Three trajectories are evaluated: one near the beginning (32-hour period), middle (6-hour period), and end (2.5-hour period). The initial conditions are taken from the aerobraking reference trajectory for the opening of the launch period.

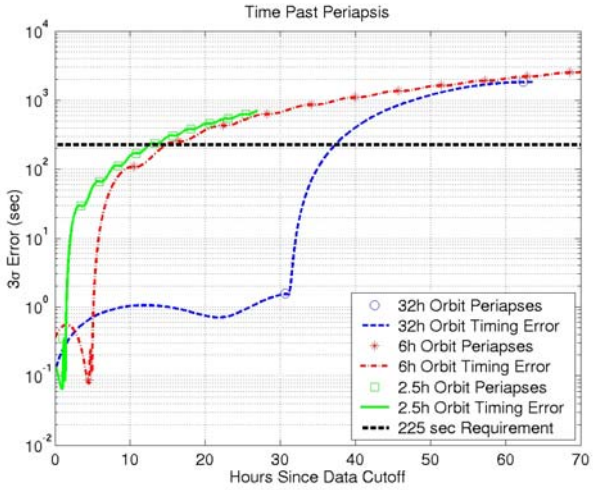

Figure 10: Periapse timing uncertainty after data cutoff

Continuous two-way Doppler tracking is simulated for the trajectories for one (32 hr), two (6 hr), or three (2 hr) subsequent periapse passes, with the trajectory propagation extending beyond for the purpose of prediction. No tracking data is collected within ±30 minutes of each periapse, and only one hour of Doppler is collected past the last periapse in the fit span. Filtering is performed using the assumptions in Table 6 through 8, and the estimated variances are mapped to the orbital element time from periapse (TFP) at the periapse passage epochs. TFP is the metric used to estimate the number of orbits past the fit span than can be predicted before the 225-second timing requirement is exceeded.

The results are shown in Fig. 10, which plots the uncertainty in periapse timing as a function of the hours since data cutoff, for all three cases examined. The 225 sec requirement is plotted as a horizontal dashed line. The plot shows that only the next periapsis can be predicted for the long-period orbits; two periapses can be predicted from the six-hour orbit, and five can be predicted from the 2.5-hour orbit. The results are summarized in Table 13 in terms of hours/days and number of orbits

Table 13: Meeting the Periapsis Requirements Since OD Cutoff

	32-hour Orbit	**6-hour Orbit**	**2.5-hour Orbit**
Hours (days)	32 hours (1.3 days)	12 hours (0.5 days)	12.5 hours (0.5 days)
Number of Orbits	1 Orbits	2 Orbits	5 Orbits
Nav Update Frequency (PTE disabled)	1Update/Day	3 Updates/Day	3 Updates/Day

meeting navigation aerobraking requirement since OD cutoff. It also includes Navigation's update frequency assuming the on-board periapsis timing estimator (PTE) disabled and four-hour process latency time. The periapse timing error is driven by the 35% 1 sigma stochastic uncertainty in atmospheric density through each periapse pass. Since the next periapse after a fit encounters little drag around apoapse, its timing can be predicted to within a few seconds regardless of the orbit period. However, the density uncertainty during each predicted pass causes an uncertainty in the resulting period reduction, and thus the timing of subsequent periapses.

The results are consistent with the performance of past aerobraking missions, such that only one rev could be predicted reliably until the orbit period decreased sufficiently, and multiple uploads per day are required during the

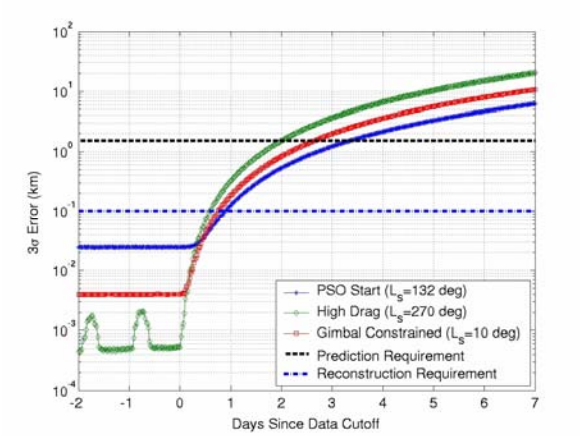

Figure 11: 3-σ Short-Term downtrack position uncertainties

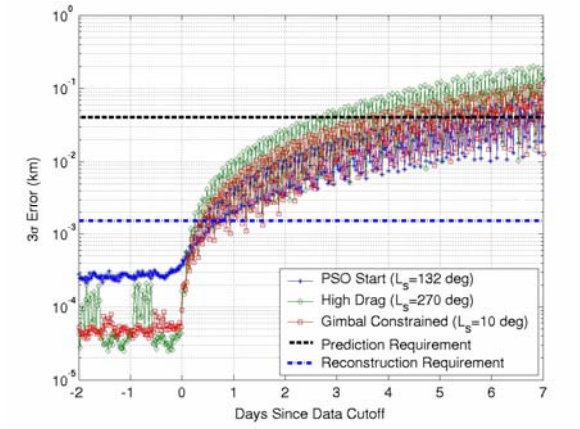

Figure 12: 3-σ Short-Term Radial position uncertainties

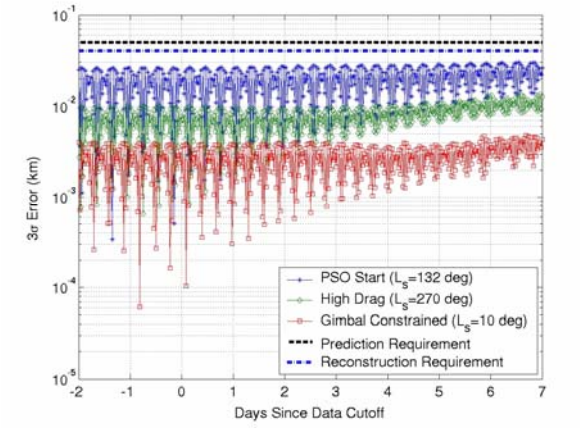

Figure 13: 3-σ Short-Term crosstrack position uncertainties

latter part of aerobraking to maintain periapse timing accuracy. Note also that the MRO project has baselined the periapse timing estimator on-board capability that was successfully demonstrated on Mars Odyssey during aerobraking. This feature allows the spacecraft to process the accelerometer data from a drag pass to estimate the periapse time. The MRO version of PTE will also employ an algorithm to predict the next periapse. Therefore, based on the covariance analysis results and past experience with PTE, navigation of MRO during aerobraking is expected to perform similarly to Mars Odyssey. It should be noted however, that MRO has more margin on the heating rates as compared to Odyssey, which will help ease stress on the flight team during operations. The latter is an important point since aerobraking is expected to last six months as compared to the 2.5 months it took for Odyssey.

3. Primary Science

Unlike previous missions, MRO spends its entire primary science phase of the mission at altitudes where the atmosphere has a substantial effect. Also, since this mission phase has the most stringent navigation requirements, it has received more attention with regard to navigation accuracies. The covariance analysis procedure used is straightforward. Starting with initial conditions for a particular time in the PSP, an orbit is propagated for 14 days. Tracking data (Doppler only for this mission phase) is collected for the first seven days using the schedule in Table 3. The filtering is performed, and the estimated variances are rotated and plotted in terms of spacecraft downtrack, crosstrack, and radial coordinate directions. For filtering, the standard assumptions listed in Table 6 through 8 are used. Estimated parameters included the state, solar radiation pressure, AMDs, gravity, and drag. The gravity field parameters were chosen as described in Section III-E. For drag, a single parameter for the drag coefficient, C_D, is used. The considered parameters included the media, Earth orientation, and station location parameters. Earth and Mars ephemeris errors were not included in the filter.

The Martian atmosphere has a strong seasonal dependence, with the seasonal boundaries defined by solar longitudes L_s = 0, 90, 180, and 270 degrees. Northern hemisphere spring begins at L_s = 0, followed by northern summer at L_s = 90, and so on. The covariance analysis was run in three seasons corresponding to PSP start (L_s = 132), northern winter (L_s = 270), and during a period of HGA gimbal constrained geometry (L_s = 10). PSP start occurs during northern summer, and the gimbal-constrained period occurs just after the start of northern spring. Because the PSP has periapsis frozen over the South Pole, MRO experiences the highest atmospheric drag during northern winter, and the lowest during northern summer, Fig. 11 through 13 show the results of the seasonal variations on the ephemeris

reconstruction and short-term prediction accuracies. The figures plot the downtrack, radial, and crosstrack position uncertainties as a function of time since data cutoff. In these plots, Day 0 is the time of data cutoff, so the uncertainties before this time are reconstruction values, while after this time are prediction values. Two horizontal dashed lines in these plots show the reconstruction and prediction requirements as well.

To summarize the results of seasonal variation sensitivities, the reconstruction (days -2 to 0) requirements are met in all cases. The worst reconstruction result is at L_s = 132 deg (PSP start), where the geometry is such that the orbit plane is nearly perpendicular to the Earth line, degrading the strength of the Doppler observable. Also, the PSP begins right after solar conjunction, so the Doppler data noise is larger than in the other cases. For prediction (days 0 to 7), the plots clearly show the seasonal dependence on the accuracies. The most stringent requirement to meet is the 1.5 km downtrack uncertainty, which is met (to the 3σ level) from between 2 and 3.5 days. As expected, the worst case is at L_s = 270 deg (southern hemisphere summer) where the atmosphere blooms from solar heating with the resulting higher densities at periapsis. Not surprisingly, the best case is L_s = 132, the one closest to southern hemisphere winter (L_s = 90).

In addition to the short-term prediction requirement, there is also a requirement on Navigation to provide a long-term ephemeris file, and whose accuracy is such that the viewing angle to surface targets does not change by more than 3 deg at the time of the final ephemeris delivery for that target. Since the imaging sequence is driven by a time of latitude crossing, such as the equator, this requirement in effect translates to a requirement on the downtrack position of the spacecraft at the time of image acquisition. The downtrack error then becomes a timing error since the ground target will move under the spacecraft due to the rotation of the planet. The limiting case will be at the equator, where ground motion is largest, and at spacecraft nadir, where the distance to the ground is shortest. Assuming an altitude of 265 km above the equator, the conversion factor is 0.0153 deg of crosstrack pointing error per 1 km of downtrack position error, so that a 196 km downtrack error equates to a 3 deg pointing error.

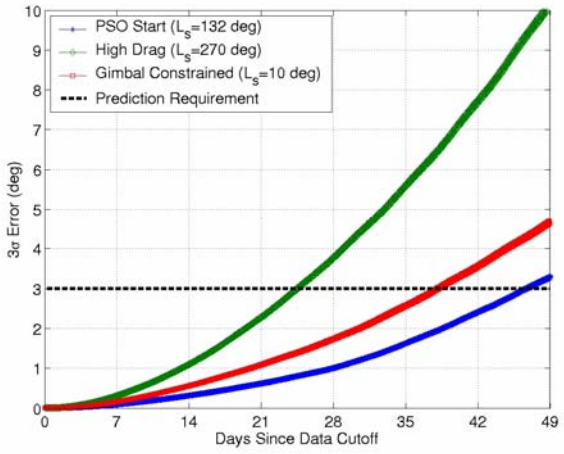

Figure 14: 3-σ Long-Term downtrack position Uncertainties

Figure 14 shows the downtrack error mapped 49 days beyond the data cutoff, with the error expressed as the equivalent off-nadir pointing angle in degrees. There is an OTM execution error of 0.02 m/s applied at 27 days after data cutoff, but it is swamped by the atmosphere uncertainty error growth.

As indicated, the predicted ephemeris error meets the 28-day, 3-deg off-nadir requirement in all but the most stressing case: the high drag season 3σ case, which reaches 3 deg in about 24 days. This implies that the requirement can be met for nearly the entire science phase, based on the assumption of a 2-day correlated atmosphere. The effect of the atmosphere uncertainty at PSP start is relatively minimized, providing an opportunity over the following months to obtain a better estimate of its long-term stochastic nature before the onset of the high drag season.

C. Navigation Primary Science Phase Operation Strategy

The major navigation responsibilities during the PSP are divided into two areas: 1) orbit determination (OD) and 2) trajectory analysis and orbit maintenance. Though these are the same processes performed in all the other mission phases, the driving requirements from the science instruments result in unique operational strategies for the PSP. Other navigation responsibilities include orbit reconstruction, model updates and trending, daily ephemeris monitoring and ΔV consumption and trending. These activities make up much of the essential background navigation functions. The output products derived from these activities are critical inputs to the engineering and science planning processes.

After the transition phase, MRO will establish in a 255 km x 320 km orbit. Atmospheric influence, reflected by the semi-major axis decay, is inevitable at such an altitude. The orbit control strategy is to maintain an adequate semi-major axis while minimizing the perturbations on the science planning, sequence generation, and navigation orbit accuracy determination processes. The advantages of this strategy not only maintain the frozen orbit, but also preserves the nature of the global repeat cycle, reduces the nominal groundtrack deviation, and simplifies the

operation complexity. Note that the OTMs are not planned for a grid-control strategy but only to maintain the frozen orbit.

This strategy is implemented through the execution of orbit trim maneuvers, utilizing the TCM thrusters. To accommodate the science process and operational simplicity, OTMs will be executed on a regular basis (nominally every 4 weeks). During low drag season, the TCM execution period can be stretched to once every 56 days subject to the limitation of the minimum OTM size. The expected OTM magnitude should range from 0.05 to 0.4 m/s. To account for the dynamic perturbation, any future OTMs will be included in the long-term and short-term ephemeris files. The OTM will be placed at mid-2nd week of the 28-day background sequence to minimize the perturbation on the science planning process. The baseline of current OTM process is to utilize a variation of nominal maneuver design process to generate mini-sequences for the execution of these burns. Typically, a full-maneuver design involves a 10-day process block, and it includes delivering a verbal burn magnitude at OTM – 10 days and a final maneuver profile file (MPF) at OTM – 7 days. However, significant influence of the atmospheric uncertainty on the OD accuracy during the PSP makes it necessary to tweak the nominal maneuver design process to reflect the ΔV update. The baseline excludes the verbal magnitude delivery at OTM – 10 days because the propulsive ΔV is small and reasonably bounded. Also the maneuver design delivered at OTM – 7 days will be a preliminary version of the burn ΔV with a fixed burn attitude. Finally, the updated burn magnitude with the fixed burn attitude (same attitude as OTM-7 day delivery) is delivered at OTM - 2 days.

Navigation long/short-term capability is described in section V-B-3. The science planning process must account for the appropriate long-term prediction uncertainty when identifying potential targets that fall within the spacecraft roll capability. The short-term ephemeris is used to generate the on-board spacecraft ephemeris file and to support the non-interactive science planning process.

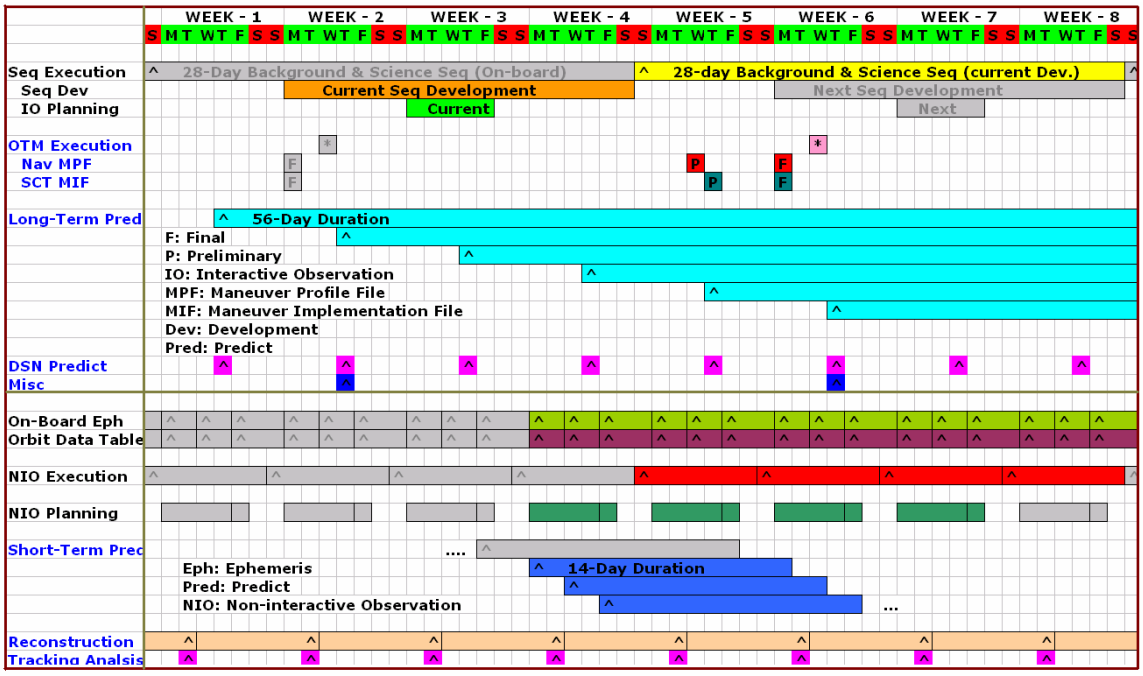

Figure 15: Navigation Product Support During Primary Science Phase

Figure 15 illustrates the navigation product support cycles and the associated science and sequence planning process for an 8-week time scale. Every week, Navigation will deliver the long-term 8-week prediction. The products are used in the generation of the background sequence to determine predicted Earth contact durations for each orbit during a DSN pass and also used by the instrument teams to select targets for the each 14-day execution cycle, and by the Mars Target Tool (MTT) for the constraint checking on the final science integrated target plan. Navigation will also deliver an 8-week predicted spacecraft ephemeris every 28 days to support the DSN selection process. Miscellaneous long-term products include the one-way light time file, maneuver design, and a long-range (> 6-month duration) spacecraft ephemeris file. In support of the on-board ephemeris and science short-range nadir observation planning process, Navigation will provide a two-week short-term prediction, at minimum, three times per week updates to the orbit prediction to meet the required prediction accuracies. Depending on the season and

atmosphere predictability, the updates may be as frequent as every day. The instrument teams use these updates in planning their non-interactive nadir observations. Other short-term products include reconstructed spacecraft ephemeris and tacking data analysis.

VI. Conclusion

Mars Reconnaissance Orbiter will be the first mission in a low Mars orbit to carry high precision imaging instruments along with other science and experimental engineering payloads. The significant amount of science data return not only helps us to gain more knowledge and understanding of our neighboring planet, but also pave the road for future Mars missions. To achieve the mission objectives, Navigation is required to satisfy, by far, the most stringent requirements compared to previous orbiter missions.

This paper has presented the dynamic modeling, trajectory and flight-path/orbit control, and orbit determination strategies capable of meeting the navigation requirements. In addition, the PSP operation plan also shows the efficiency of orbit-maintenance strategy. More importantly, to fulfill the navigation commitments, the operation strategy is flexible to accommodate any unanticipated environments.

Acknowledgments

This work was carried out at the Jet Propulsion Laboratory, California Institute of Technology, Pasadena, California under contract to the National Aeronautics and Space Administration. The authors would like to thank the support of Mars Reconnaissance Orbiter Project, Lockheed-Martin Space Systems, and Navigation and Mission Design Section.

References

[1] M. D. Johnston, et al., "The Mars Reconnaissance Orbiter Mission", 2004 IEEE Aerospace Conference, Big Sky, WY, 6-13 March 2004.
[2] R. E. Lock, P. Xaypraseuth, et al., " The Mars Reconnaissance Orbiter Mission Plan", 14th AAS/AIAA Space Flight Mechanics Conference, Maui, Hawaii, 8-12 February 2004.
[3] C. Allen Halsell, A. L. Bowes, et al., "Trajectory Design for the Mars Reconnaissance Orbiter Mission", 13th AAS/AIAA Space Flight Mechanics Meeting, Ponce, Puerto Rico, 9-13 February 2003.
[4] S. K. Wong, T. H. You, et al., "Navigating through the Venus Atmosphere", AAS/AIAA Spaceflight Mechanics Meeting, Cocoa Beach, FL, 14-16 February 1994.
[5] M. D. Johnston, P. B. Esposito, et al., "Mars Global Surveyor Aerobraking at Mars", AAS/AIAA Astrodynamics Specialist Conference, Monterey, CA, 9-11 February 1998.
[6] J. C. Smith and J. L. Bell, "2001 Mars Odyssey Aerobraking", AAS/AIAA Astrodynamics Specialist Conference, Monterey, CA, 5-8 August 2002.
[7] E. M. Standish, "Recommendation of DE405 for 2001 Mars Surveyor and for Cassini", JPL Interoffice Memorandum, 312.F-00-107, October 18, 2000 (unpublished)
[8] E. M. Standish, "JPL Planetary Ephemeris DE410", JPL Interoffice Memorandum, 312.N-03-009, April 24, 2003 (unpublished)
[9] M. Carlton, "Multiple Views of Ground Data Systems Based on Mars Reconnaissance Orbiter's GDS", SpaceOps 2004 Conference, Montreal Canada, 17-21 May 2004
[10] R. Georgevic, "Mathematical Model of the Solar Radiation Force and Torque Acting on the Components of a Spacecraft", Technical Memorandum 33-494, Jet Propulsion Laboratory, October 1, 1971.
[11] R. F. Sunseri, "Orbit Determination Program Description". Technical Report, JPL (unpublished)
[12] C. G. Justus and D. L. Johnson, "Mars Global Reference Atmospheric Model 2001 Version (MarsGRAM 2001): Users Guide", NASA/TMN2001D210961, April 2001.
[13] G. W. Rosborough, "Satellite Orbit Perturbations Due to the Geopotential", Ph.D. Thesis, 155 pp., The University of Texas, Austin, January 1986.
[14] G. J. Bierman, "Factorization Methods for Discrete Sequential Estimation", Academic Press, New York, NY, 1977.